Geometrical errors and their uncertainty in goniophotometers:
an application to road surface photometry

Geometrical errors and their uncertainty in goniophotometers: an application to road surface photometry

Johanna Bernasconi[1], Peter Blattner[1], Mikael Lindgren[2], Dominique Renoux[3], and Paola Iacomussi[4]

[1]*METAS, Bern Switzerland*
[2]*RISE, Borås, Sweden*
[3]*LNE Paris, France*
[4]*INRIM, Torino, Italy, p.iacomussi@inrim.it*

ABSTRACT: The measurement of luminance spatial distribution of road surfaces provides a full description of the light-material interaction. This quantity is related to road lighting system design and its measurement is performed by goniophotometers. Uncertainty analysis of goniophotometers is usually performed on laboratory instruments with very low beam divergence. Road surface luminance uncertainty budget needs a detailed approach because samples are large and due to the size constraints of on-site measurements, portable instruments tend to have larger beam divergence. In addition, due to the nature of samples, the uncertainty depends on the sample under test. The paper investigates the geometrical errors implicit in luminance measurements made by goniophotometry in the road surface analysis. It presents a theoretical model of a goniophotometer for spatial luminance distribution and provides an evaluation of errors dealing with sensors and source optics characteristics necessary to assess the uncertainty budget of the measurement results.

Keywords: Aperture effects, luminance measurements, Uncertainty budget, road surface, luminance coefficient, *r*-tables, BRDF.

Received January 1, 20213; **In final form** January 31, 20213; **Published** June 20213

Corresponding author: Paola Iacomussi, e-mail: p.iacomussi@inrim.it

1. INTRODUCTION

The luminance coefficient of a material is the ratio between the luminance reflected by the material and the illumination from the light source. The knowledge of luminance coefficients of road pavements allows the design of road lighting systems that ensure road safety, while saving energy and complying with the different normative requirements. The luminance coefficient spatial distribution for generic materials is called BRDF (Bidirectional Reflectance Distribution Function) and it is a function of four angles. Two angles identify the lighting direction and two the observation direction. In road surface analysis, the BRDF is simplified and limited to a few lighting directions and only one observation direction, and the values are tabulated (so-called *r*-tables) [1], [2].

Thanks to *r*-table values is it possible to link the intensity emission in a given direction of a road lighting luminaire to the luminance perceived by a driver in a reference position on the road [3]. This approach ensures that the design of road lighting systems (geometries and spacing) is able to fulfil normative requirements, in terms of visibility, to ensure road user's safety.

The entire design approach is based on the knowledge of *r*-tables of the road surfaces: there are reference *r*-tables that can be used, or it is possible to measure on site the *r*-tables of actual asphalt. Due to the geometry of measurement, the luminance coefficient must be known with a high angular resolution. This is true for both the driver's observation direction and all the lighting directions [1], [2]. Specialized goniophotometers have therefore been designed to measure, on site or in laboratory, the luminance coefficient measurements of road pavements. The instruments feature different optical and geometrical characteristics [4], which impact the measurement uncertainty. From this deviation from a perfect measurement geometry, originates an error which we call aperture effect: the paper shows that these geometrical contributions are crucial in the measurement of the luminance coefficient and in its uncertainty determination, especially for on-site measuring devices. The main geometrical factors of influence are the lighting direction and collimation, the illuminated and observed areas, the observation direction and angular field of view. The contribution

due to the aperture effect can be determined and corrected, since it is a systematic error. However, some uncertainties are associated with the correction of this effect. In addition, alignment errors of the systems contribute to the total uncertainty.

2. METHODS

2.1. Luminance coefficient

According to the International Lighting Vocabulary [4], the luminance coefficient, q, is defined as the ratio of the luminance L in a given direction at a point on the surface, to the horizontal illuminance E, at the same point (definition no. 17-24-079 in [4]). Under specified illumination conditions depending on the targeted normative requirements [3], [5] we obtain:

$$q = q(\alpha, \delta, \beta, \varepsilon) = \frac{L(\alpha,\delta)}{E(\beta,\varepsilon)}, \quad (1)$$

where:

- α, δ are the angles of the observation direction,
- β, ε are the angles of the illumination direction,
- L is the measured luminance in the α, δ direction,
- E is the measured illuminance provided from the β, ε direction.

The angle α is measured vertically from the horizontal plane of the sample to the observer position and δ laterally between the observation direction and the reference direction of the sample. δ is set to zero because road surfaces present isotropic behaviour. The angle ε is measured from the vertical to the direction of illumination and β is the angle between the vertical planes containing the illumination direction and the observation direction. The geometry is described in figure 4 of [6] for the specific case of road surface measurements, as defined in the European road lighting standard series EN 13201. This coefficient is a four-dimensional quantity, measured in sr^{-1}. In the application to road surface luminance coefficient evaluation, the reduced luminance coefficients $r(\alpha, \delta, \beta, \varepsilon) = q \cdot \cos^3\varepsilon$ are usually used. The values are determined for specific observation angles ($\alpha = 1°$, isotropy in δ) and specific illumination angles ($0 \leq \tan\varepsilon \leq 12$, $0° \leq \beta \leq 180°$) and the values are usually presented in a so-called *r*-table.

A number of *r*-tables, representative of road surface behaviour, can be found in the technical report CIE 066:1984 [1] for reference.

2.2. Measuring instruments for *r*-tables

A deep review of all available instruments for road surface luminance coefficient measurements is available in [5]. These systems can be categorized in two groups of instruments:

- instruments which have collimated or telecentric illumination and detection systems with very low beam divergence,
- instruments without optics or with imaging optics for the illumination and/or the detection.

All instruments suffer from uncertainties in the positioning and the alignment of the system. The most important elements are the position of the light source and its illumination angle, the position and tilt of the sample under consideration, the position and angle of the detection system. The first category of instruments, due to their very low beam divergence, are not subject to aperture effects. The second category is subject to an aperture effect, which depends on the aperture sizes and angles of the illumination and detection system. This effect is investigated in this paper. It yields a systematic error, k_A, which can be corrected similarly to other systematic errors due to straylight, temperature variations, nonlinearity of the detector, etc.

2.3. Aperture effects

Considering the luminance coefficient definition, the illuminance should be measured at the same point of luminance with the incident light originating from one of the specific directions listed in the *r*-table. In practice, this is not possible since the lighting system and the luminance detector have extended apertures to emit and collect light as shown in Figure 1. As a result, the measured luminance and illuminance are an average over an extended area in a range of angles. Additionally, measured samples like road surfaces, can be highly nonuniform, hence the luminance coefficient will vary at each point and the average across a certain surface is recorded.

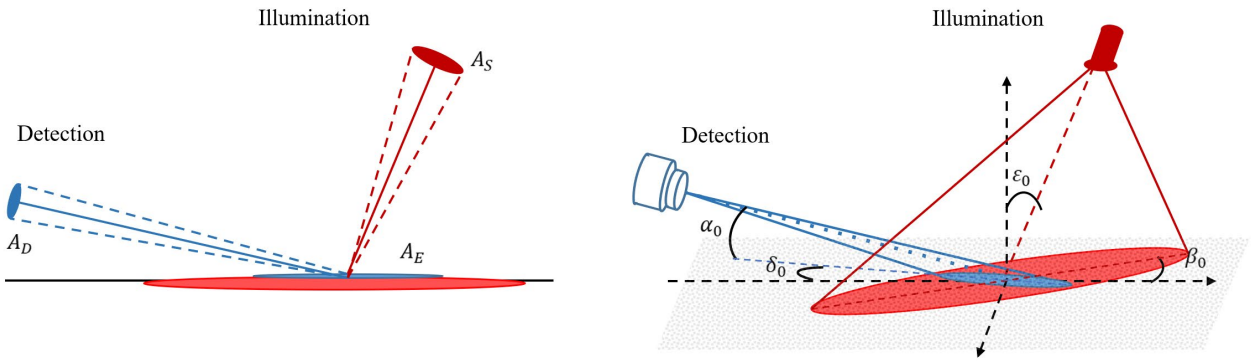

Figure 1. A schematic of the geometrical effects with left) apertures of the illumination A_S with coordinate system (x_S, y_S), of the detection A_D with coordinate system (x_D, y_D) and of the effective illuminated area A_E with coordinate system (x_E, y_E); right) the nominal angles (α_0, δ_0) of the detector and (β_0, ε_0) of the source.

Due to the extended apertures and illumination areas, the measurement system suffers from different systematic effects. Considering the lit area, the actual incident angles (β_E, ε_E) differ from the nominal values (β_0, ε_0) (Figure 1) and vary inside the effective illumination field, A_E, and depends also on the aperture of the lighting source, A_S.

Similar considerations are also valid for the viewing detector: the detection angles (α_D, δ_D) differ from the nominal values (α_0, δ_0) (Figure 1) and vary across the detection field, A_D.

In the ideal case of luminance meters with binary behaviour, only radiation within the field of detection A_D is measured and the detector sensitivity across the field is constant. However, in practice the detector sensitivity may vary slightly across the surface of the detector itself, $k_D(x_D, y_D)$.

In the ideal case, the illuminance field is perfectly homogenous and no light is outside the nominal field, but in practice the illumination field is not homogenous, i.e. $E = E(x_E, y_E)$.

Considering all the aforementioned effects, the collected signal of the luminance detector, L_D differs from the luminance of a perfect instrument L_0, because of the aperture effects of both lighting source, detector, and the spatial sensitivity behaviour of the detector into the different fields;

$$L_D = k_A(\alpha_0, \delta_0, \varepsilon_0, \beta_0)\, L_0 = k_A(\alpha_0, \delta_0, \varepsilon_0, \beta_0) q(\alpha_0, \delta_0, \varepsilon_0, \beta_0) E_0 k_{D0}. \quad (2)$$

L_D can also be expressed as a combination of the actual luminance coefficient of the sample $q(\alpha_D, \delta_D, \beta_E, \varepsilon_E)$ and the illuminance on the sample point, $E(x_E, y_E)$, considering the appropriate integration areas (the extended fields in Figure 1)

$$L_D = \frac{1}{A_D \cdot A_E \cdot A_S} \cdot \iint_{A_D} \iint_{A_E} \iint_{A_S} q(\alpha_D, \delta_D, \beta_E, \varepsilon_E) E(x_E, y_E)\; k_D(x_D, y_D), \quad (3)$$

where:

- A_D is the detection field,
- A_E is the illumination field,
- A_S is the aperture of the lighting source,
- (α_D, δ_D) are the actual detection angles,
- (β_E, ε_E) are the actual incident angles,
- (x_E,y_E) are the coordinates in the illumination field A_E,
- E is the illuminance in the illumination field,
- (x_D,y_D) are the coordinates in the detector field A_D,
- k_D is the sensitivity of the detector that varies across A_D.

The calculation of L_D of Eq. (3) can be done either by integration of the sixfold integral or by the Monte Carlo method.

To evaluate k_A through simulation, it is essential that the luminance coefficients q are known also at angles around the nominal directions $(\alpha_0, \delta_0, \varepsilon_0, \beta_0)$. However, in road lighting, they are known in only very limited directions, given by the r-tables.

It is therefore essential to build a general four-dimensional model of the BRDF. Road samples are considered isotropic; hence the values do not change as a function of the δ angle.

3. RESULTS

The aperture effect depends on the type of measured sample: to correctly evaluate the impact of the systematic behaviour of goniophotometers subjected to aperture effects, a mathematical model of BRDF samples must be developed to understand the metrological capabilities of the measuring device. Unfortunately, the BRDF (or q) is the quantity under investigation, so it is difficult to predict the model. Starting from CIE published reference tables to generate BRDF values, two ways are possible: interpolation or modelling. A mathematical model is much faster than the interpolation method and it overcomes the difficulty in interpolating around specular peaks.

3.1. BRDF Model

One of the simplest BRDF models is a combination of the perfect diffuse model of a Lambertian sample (with constant luminance), with the scattered specular Phong model [7]. The Phong model is based on the cosine of a given angle, elevated to a given power, which gives the sharpness of the specular reflection. The given angle is the angle between the observation direction and the specular reflection direction. The output of this simple model, well-used in basic physical 3D-rendering engines, can be compared, under the form of solid *r*-tables, in Figure 2 with a reference pavement reflectance (C2) given in CIE 066:1984 [1]. The top pane represents the basic model and the bottom pane the actual behavior of a C2 pavement. It can be observed from this figure, but it happens also for other reference pavements, that the two 3D shapes of BRDF have significant differences.

Additional BRDF models exist but have very limited applications [8], [9], which do not give satisfactory results for road surface pavement. On the contrary, good results have been obtained implementing the aforesaid basic model with supplementary experimental components, as a function with adjustable parameters. Five different road-surface *r*-tables have been modelled: four CIE reference pavements (R1, C2, R3, R4) and a measured sample. The *r*-tables have been chosen with different specular indices S_1 to represent the range of realistic road pavements BRDF, with S_1 values equal to 0.25, 0.93, 1.11, 1.49 and 0.39. Sharp changes in measured *r*-tables have been observed experimentally for small changes of α with

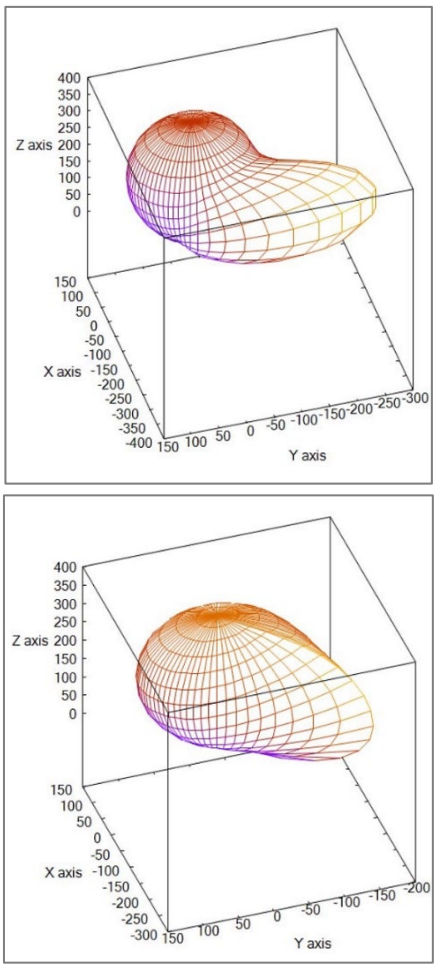

Figure 2. The top pane represents the basic model and the bottom pane the actual behaviour of a C2 pavement.

road pavements measured with laboratory goniometers [10].

This can be partly understood because of masking effects due to the surface roughness. For this reason an additional component, applied as a configurable attenuation factor for grazing angles, has been added to the model to account for this masking effect. In addition, a component representing small scattered retroreflection behaviour was included in a modified Phong model.

Finally, the BRDF behavior of reference road surfaces can be expressed as:

$$BRDF(\theta_i, \varphi_i, \theta_r, \varphi_r) = \Big(k_{\text{diff}} + k_{\text{phong}} \cdot (\cos\Omega)^r + k_{\text{phong-retro}} \cdot (\cos\Omega')^s + k_{\text{exp}} \cdot f(\varepsilon)^p \cdot \left(\frac{\pi-\beta}{\pi}\right) \exp(1 + h \cdot f(\varepsilon)^2)\Big) \cdot g(\theta_i) \cdot g(\theta_r)/g(\theta_r^*), \quad (4)$$

where the nature of components and their corresponding mathematical expressions of terms are presented in Figure 3.

Model components	Mathematical expression	Parameters
diffuse (constant)	k_{diff}	
scattered specular (Phong model) [8]	$k_{phong} \cdot (\cos\Omega)^r$	$\cos\Omega = \cos\theta_i \cdot \cos\theta_r - \sin\theta_i \cdot \sin\theta_r \cdot \cos(\varphi_i - \varphi_r)$ θ_i, θ_r polar incident and reflected angles, equal to 0 at zenith and $\leq \pi/2$ φ_i, φ_r azimuthal incident and reflected angles, φ of detector centre is 0
experimental based on an artificial function of incident angles (ε, β)	$k_{exp} \cdot f(\varepsilon)^p \cdot \left(\frac{\pi - \beta}{\pi}\right) \exp(1 + h \cdot f(\varepsilon)^2)$	$\varepsilon = \theta_i \cdot \theta_r / {\theta_r}^*$ θ_r^*: polar observation angle of fitted *r*-tables (89°) $\beta = \lvert\varphi_i - \varphi_r - \pi\rvert$ $f(\varepsilon) = \sin\varepsilon \cdot \frac{\cos\varepsilon}{(\cos\varepsilon)^2 + \mu}$
global attenuation factor for grazing angles of incidence or observation	$g(\theta_i) \cdot g(\theta_r)/g(\theta_r^*)$	$g(\theta) = \begin{cases} (a \cdot \theta^2 + b \cdot \theta + c)^t, & \text{for } \theta > \theta_l, \\ 1, & \text{for } \theta < \theta_l, \quad \theta_l > 85.3° \end{cases}$
scattered retro-reflected (modified Phong model)	$k_{phong-retro} \cdot (\cos\Omega')^s$	$\cos\Omega' = \cos\theta_i \cdot \cos\theta_r + \sin\theta_i \cdot \sin\theta_r \cdot \cos(\varphi_i - \varphi_r)$

Figure 3. Model components and the corresponding mathematical expressions.

The objective is not to get the same *r*-table values as the considered reference from the BRDF model, but rather to get simulated data representative of realistic BRDF for uncertainty assessment. It is especially important to get similar shape of the specular component, which is the main contributor to the *aperture effect* error. The overall match is very good for the five selected references. The maximal deviation is within ±9 % of the maximal *r*-value. The root mean square deviation is within 2.6 % of the maximal *r*-value. As all the components are not based on physical principles but derived from *r*-tables, the simulated BRDF can only be used for small variations around $\alpha = 1°$ for which the *r*-tables are provided and as commonly done for uncertainty evaluation.

4. DISCUSSIONS

4.1. Aperture effect evaluation

The *aperture effect* is considered for any defined geometries and optical systems, by means of a numerical integration of all the possible rays: each ray emitted from the light source, incident on a sample point and reflected toward a point of the detector sensitive field, is weighted by the modelled BRDF at that point. The difference between the integrated modelled BRDF and the modelled BRDF is computed and represents a systematic error. Since this effect strongly depends on the incident angle (ε_0, β_0), the aperture effect is calculated for each incident direction. The systematic error due to the aperture effect can be corrected by means of a relative measurement with a reference close to the targeted sample. The reference is used to determine the correction factor k_A of eq. (2). The whole process is available by a freely available software LUMCORUN developed during the SURFACE project [11] (a Euramet funded project) and downloadable from the project repository [12].

The uncertainties on the angles originate from the positioning uncertainties of the goniometer and the misalignment of the sample. It should be noted that, in principle, there is no correlation between these inputs and the aperture effects.

For the evaluation of the uncertainty budget in luminance coefficient or BRDF measurement, a full measurement model able to include all variables of influences should be developed [13], [14]. When the model is too complex, a Monte Carlo Method (MCM) to quantify the resultant uncertainty on the measurand should be used. Without aperture effect, a loop over a large number (typically 5000-50000)

generates random angles of specified standard deviations and distributions. Those angles are then used to compute the standard deviation of the outcomes, i.e. the values of the BRDF model for comparison with the *r*-tables.

The comparison was done for an actual road surface, measured by an on-site goniophotometer, choosing the reference *r*-table closest to the sample behaviour to calculate the impact of the aperture effect uncertainty. The results displayed in Figure 4 are the calculated systematic errors.

For most of the table, the software result is consistent with the measurement and the software highlights the error for β between 0° and 10°. Without any calibration, the error can be very large for specular samples. By calibrating the measurement with the portable instrument with a sample of similar characteristics, the aperture effect can be greatly diminished, the accuracy of the results being determined by how similar the sample under test and the calibration sample are. It is also possible that the straylight from the measurement is higher than what is corrected for, when the light source is illuminating the sample at grazing angles and toward the detector. The results show that the software evaluation also highlights errors which are different from the aperture effect. In particular, the alignment uncertainty adds an uncertainty in some directions, which might compensate some of the errors, or on the contrary, enlarge the errors. The illumination directions with $\beta \leq 20°$ and $\varepsilon \geq 70°$ show the largest values, which corresponds with the peak of the sample BRDF.

5. CONCLUSIONS

A model of the geometrical errors in gonio-photometric measurement was developed. It was implemented in software (LUMCORUN) that includes the modelling of the geometry of the instrument and the modelling of the behaviour of the sample under test. The model of the BRDF of the sample consists of a diffuse, a specular and an experimental component as well as additional components to fit experimental data, for retro-reflection and grazing angles effect.

A comparison between the results obtained with the software and measurements by a portable goniophotometer was made. Illumination directions corresponding to specular reflection toward the detector provides large systematic errors.

tanε/β(°)	0	2	5	10	15	20	25	30	35	40	45	60	75	90	105	120	135	150	165	180
0	1.02	1.02	1.02	1.02	1.02	1.02	1.02	1.02	1.02	1.02	1.02	1.02	1.02	1.02	1.02	1.02	1.02	1.02	1.02	1.02
0.25	1.03	1.03	1.03	1.02	1.02	1.01	1.01	1.01	1.01	1.01	1.01	1.02	1.02	1.02	1.02	1.02	1.02	1.02	1.02	1.02
0.5	1.04	1.04	1.03	1.02	1.01	1.01	1.01	1.01	1.01	1.01	1.02	1.02	1.02	1.02	1.02	1.02	1.02	1.02	1.02	1.02
0.75	1.05	1.05	1.03	1.01	1.00	1.01	1.01	1.01	1.01	1.01	1.02	1.02	1.02	1.02	1.02	1.02	1.02	1.02	1.02	1.02
1	1.06	1.05	1.02	1.00	1.00	1.00	1.01	1.01	1.01	1.01	1.02	1.02	1.02	1.02	1.02	1.02	1.02	1.02	1.02	1.02
1.25	1.06	1.05	1.01	0.99	0.99	1.00	1.01	1.01	1.01	1.02	1.02	1.02	1.02	1.02	1.02	1.02	1.02	1.02	1.02	1.02
1.5	1.07	1.06	1.01	0.98	0.99	1.00	1.01	1.02	1.02	1.02	1.02	1.02	1.02	1.02	1.02	1.02	1.02	1.02	1.02	1.03
1.75	1.08	1.06	1.01	0.98	1.00	1.01	1.02	1.02	1.03	1.03	1.03	1.02	1.02	1.02	1.02	1.02	1.02	1.02	1.03	1.03
2	1.09	1.06	1.00	0.98	1.00	1.02	1.03	1.03	1.03	1.03	1.03	1.02	1.02	1.02	1.02	1.02	1.02	1.02	1.03	1.03
2.5	1.12	1.08	1.00	0.98	1.02	1.04	1.04	1.04	1.03	1.02	1.02	1.01	1.02	1.02	1.02	1.02	1.02	1.02	1.03	1.03
3	1.17	1.12	1.01	0.99	1.04	1.04	1.03	1.01	1.00	1.00	1.00	1.01	1.02	1.02	1.02	1.02	1.02	1.02	1.03	1.04
3.5	1.25	1.17	1.02	0.99	1.02	1.01	0.99	0.98	0.97	0.98	0.99	1.01	1.02	1.02	1.02	1.02	1.02	1.02	1.03	1.04
4	1.36	1.24	1.03	0.95	0.97	0.95	0.94	0.95	0.96	0.98	0.99	1.02	1.02	1.02	1.02	1.02	1.02	1.03	1.04	1.04
4.5	1.51	1.34	1.02	0.88	0.90	0.90	0.91	0.94	0.97	0.99	1.00	1.02	1.02	1.02	1.02	1.02	1.02	1.03	1.04	1.04
5	1.68	1.44	1.00	0.80	0.84	0.86	0.90	0.94	0.97	0.99	1.01	1.02	1.02	1.02	1.02	1.02	1.02	1.03	1.04	1.04
5.5	1.86	1.55	0.96	0.71	0.78	0.84	0.91	0.96	0.99	1.00										
6	2.07	1.68	0.90	0.62	0.74	0.84	0.92	0.97	1.00											
6.5	2.46	1.94	0.86	0.55	0.73	0.88	0.97	1.02												
7	2.64	2.03	0.79	0.48	0.73	0.90	0.99	1.04												
7.5	2.84	2.13	0.74	0.43	0.73	0.91	1.01													
8	3.12	2.28	0.68	0.39	0.75	0.94	1.03													
8.5	3.50	2.50	0.66	0.38	0.80	1.02	1.11													
9	3.66	2.55	0.59	0.36	0.82	1.04														
9.5	3.78	2.59	0.53	0.35	0.84	1.05														
10	3.92	2.63	0.47	0.34	0.86	1.07														
10.5	4.11	2.70	0.43	0.33	0.88	1.08														
11	4.30	2.81	0.40	0.33	0.90	1.10														
11.5	4.73	3.06	0.39	0.34	0.99															
12	4.81	3.08	0.35	0.34	1.01															

Figure 4. Ratio k_A of the results from the software with "ideal" and non-ideal instruments.

The process highlighted the high dependency of the results on the type of sample used and reference table used to model BRDF. To increase accuracy of the modelling and of the uncertainty evaluation, a good database of up-to-date reference *r*-tables is required.

Thanks to the simulation, it is possible to predict some of the instrument behaviours and therefore, in the future, to correct the systematic effects due to the aperture.

The evaluation by the software can also be used to determine the uncertainty due to the misalignment.

The developed software is a big step towards a better modelling of luminance coefficients and BRDF measurement and is therefore an important tool for the establishment of more accurate uncertainty budgets.

ACKNOWLEDGEMENT

This research has been conducted in the project 16NRM02 SURFACE and has received funding from the EMPIR programme co-financed by the Participating States and from the European Union's Horizon 2020 research and innovation programme.

REFERENCES

[1] Road surfaces and lighting (joint technical report CIE/PIARC), CIE 066:1984.
[2] Road surface and road marking reflection characteristics, CIE 144 :2001
[3] Road lighting - Part 3: Calculation of performance, EN 13201-3:2015.

[4] International Lighting Vocabulary CIE S 017/E:2011.
[5] Road lighting - Part 2: Performance requirements, EN 13201-2:2015.
[6] V. Muzet, J. Bernasconi, P. Iacomussi, S. Liandrat, F. Greffier, P. Blattner, J. Reber, and M. Lindgren, "Review of road surface photometry methods and devices – Proposal for new measurement geometries, LRT 1–16 (2020).
[7] E. P. Lafortune and Y. D. Willems, Using the Modified Phong Reflectance Model for Physically Based Rendering" Report CWP197 (Departement Computerwetenschappen, KU Leuven, 1994).
[8] Alexander Basov, Development of a goniophotometer for measuring reflective properties of road surfaces, Master Thesis, (Lappeenranta University of Technology, 2017).
[9] Korobko A.A., Approximation of road surface luminance coefficient, in Proceedings of the CIE Centenary Conference (CIE x038:2013), pp. 1076–1082.
[10] R. B. Gibbons, Influence of Pavement Reflection on Target Visibility, Ph. D dissertation, (University of Waterloo, 1997).
[11] SURFACE consortium, 16NRM02 SURFACE website, https://surface-nrm02.eu, accessed 2023.
[12] D. Renoux, "LUMCORUN", Zenodo (2021), https://doi.org/10.5281/zenodo.5547682.
[13] ISO/IEC Guide 98-3:2008, https://www.iso.org/cms/render/live/en/sites/isoorg/contents/data/standard/05/04/50461.html.
[14] ISO/IEC Guide 98-3:2008/SUPPL1:2008," https://www.iso.org/cms/render/live/en/sites/isoorg/contents/data/standard/05/04/50461.html.